Heavy impurity transport in tokamaks with plasma flows and saturated 3D perturbations

E. Neto[1], J. P. Graves[1], M. Raghunathan[2], S. Lanthaler[1], D. Pfefferlé[3], W. A. Cooper[4], C. Sommariva[1] and JET contributors *

[1] *École Polytechnique et Fédérale de Lausanne, Swiss Plasma Center, Lausanne, Switzerland*

[2] *Institute For Plasma Research, Ahmedabad, India*

[3] *University of Western Australia, Crawley, Australia*

[4] *Swiss Alps Fusion Energy (SAFE), Switzerland; retired from École Polytechnique et Fédérale de Lausanne*

Observations in JET hybrid scenarios show that early termination of the plasma can be caused by tungsten accumulation events, sometimes preceded by long living MHD perturbations [1]. Of concern in this work are non-resonant $1/1$ kink modes, though it has been observed that NTM islands also cause impurity accumulation [2]. Here we report on work done to understand the effect of ideal 3D saturated MHD ($1/1$ kink) and strong flows on heavy impurity transport. Previously [4] $1/1$ kink modes and toroidal rotation were consider in the Pfirsch-Schlüter regime. We generalize this work to include self consistent neo-classically resolved 3D flows, and associated electrostatic potential due to asymmetries in the Pfirsch-Schlüter and banana regimes. An implementation of the 3D centrifugal effects and 3D electrostatic potential correction on the VENUS-LEVIS code [3], based on neoclassical 3D flow theory in [5] and guiding center theory in [6], is presented in this work. Simulations are performed to study this phenomena in both high (Pfirsch-Schlüter) and low (banana) collisionality regimes for background ions in order to understand the impact of saturated 1/1 internal kink mode on the peaking of tungsten distributions in JET hybrid scenarios exhibiting continuous 1/1 activity. Two VMEC equilibria (see figure 1) are obtained which are identical except for the fact that one is axisymmetric while the other one is a 3D equilibrium which models a 1/1 internal kink mode similar to the one observed in the JET pulse #92181. The pressure, density and temperature profiles used to obtain these equilbria were also taken from the experimental data. The axisymmetric equilibrium is used to model the early state of the plasma where the 1/1 kink mode is not yet present. Having determined the magnetic equilibrium geometry we can then proceed to calculate the 3D neoclassical flows. This can be achieved using the model proposed in [5]. We then assume the

*See the author list of "Overview of the JET preparation for Deuterium-Tritium Operation" by E. Joffrin et al. to be published in Nuclear Fusion Special issue: overview and summary reports from the 27th Fusion Energy Conference (Ahmedabad, India, 22-27 October 2018)

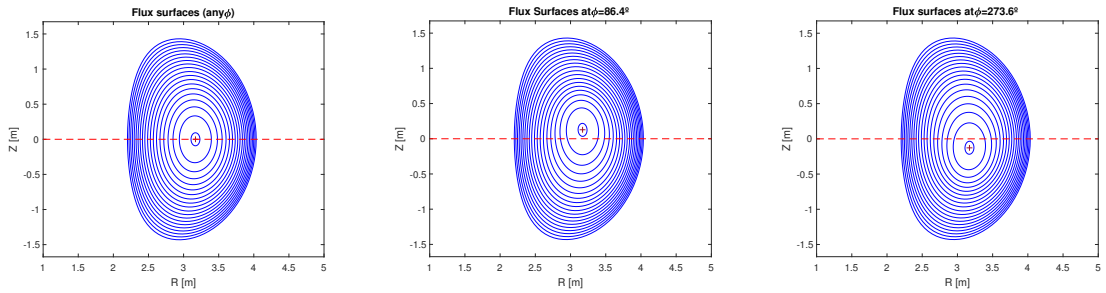

(a) *Axisymmetric equilibrium at any toroidal angle* ϕ

(b) *1/1 kink at the toroidal angle* $\phi = 86.4°$

(c) 1/1 kink at the toroidal angle $\phi = 273.6°$

Figure 1: *Flux surfaces of the two MHD equilibria obtained from VMEC.*

background ions zeroth order perpendicular flow is given by

$$\vec{U_{\perp_I}} = \frac{\vec{B}\times\vec{\nabla}\Phi_0(\psi)}{B^2} + \frac{\vec{B}\times\vec{\nabla}P_I(\psi)}{B^2 q_I N_I(\psi)}, \tag{1}$$

where $\vec{B}$ is the magnetic field and Φ_0 is the electric field, q_I the background ion charge, P_I is the ion pressure and N_I the ion density. ψ is the flux coordinate chosen for the set of flux coordinates (ψ,θ,ϕ). One can then obtain the parallel component of the flow

$$\vec{U_{\parallel_I}} = -\left(\frac{g_2}{B^2} - \frac{\langle g_2\rangle}{\langle B^2\rangle}\right)\left[\Phi_0'(\psi) + \frac{P_I'(\psi)}{q_I N_I}\right]\vec{B} + \frac{\langle U_{\parallel_I} B\rangle}{\langle B^2\rangle}\vec{B}. \tag{2}$$

In these expressions $\langle X\rangle$ stands for flux average of the quantity X and $X' = \frac{dX}{d\psi}$ and $g_2(\psi,\theta,\phi)$ is a geometrical factor obtained from the continuity equation which depends only on the magnetic geometry. The bootstrap part of the flow is given by

$$\frac{\langle U_{I_\parallel} B\rangle}{\langle B^2\rangle} = -\frac{G_C(\psi)}{\langle B^2\rangle}\left[\Phi_0'(\psi) + \frac{P_I'(\psi)}{q_I N_I} + C_\mu \frac{T_I'(\psi)}{q_I}\right], \tag{3}$$

where $G_C(\psi)$ is a geometric factor, C_μ is the ratio between viscosity coefficients and T_I is the temperature of the ions. Both G_C and C_μ depend on the collisional regime, being different for the Pfirsch-Schlüter (high collisionality) regime and the banana (low collisionality) regime and their expressions can be seen in sections 9.1.1 (Pfirsch-Schlüter) and 9.3 (banana) of [5]. The electrostatic potential correction Φ_1 due to 3D effects is obtained from solving quasi-neutrality and

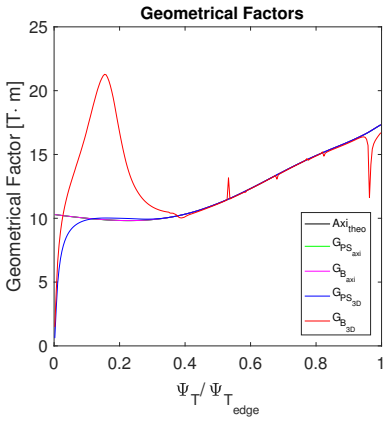

Figure 2: *Geometrical factors for the equilibria showed in 1.*

$$\vec{B}\cdot\vec{\nabla}\Phi_1(\psi,\theta,\phi) = -\frac{m_I T_I(\psi)}{e(Z_I T_e(\psi) + T_I(\psi))}\{\vec{U_I}\cdot\vec{\nabla}\vec{U_I}\}, \tag{4}$$

which only depends on the background ion flow and on the magnetic geometry. Here, Z_I is the charge number of the background ions. Therefore, both the flow and the electrostatic potential correction are determined by the magnetic geometry and experimental profiles (pressure,

temperature and density), and can be computed numerically for a given 3D magnetic equilibrium. However, an analytical solution to these equations exists in axisymmetry and therefore the numerical solver can be robustly tested in the axisymmetric case. In the axisymmetric case $G_C = G_{PS} = G_B = G_{theo}$, in which PS stands for Pfirsch-Schluter regime and B for banana regime, and the contravariant component of the poloidal $E \times B$ flow ($U^{\theta}_{\vec{E}\times\vec{B}}$) should vanish. Figures 2 and 3 show the numerical solutions of these quantities for the equilibria showed in 1 against the analytical axisymmetric solution, with ψ_T the toroidal flux. We see that the axisymmetric conditions are verified with a small error. Hence, we benchmark the solver in the axisymmetric case. While there is not an analytical solution we can see that for large ψ_T (where the 3D equilibrium is almost axisymmetric) the 3D solutions are identical to the axisymmetric ones. Hence, this background ion flow, as well as the electrostatic potential correction and the magnetic equilibrium, can be used as a background equilibrium to follow tungsten in an internal kinked $1/1$ plasma (similar to the JET pulse #92181) with the Venus-Levis code. Simulations were done using the background already described.

The Venus-Levis code was modified to include the 3D centrifugal corrections due to the strong $E \times B$ flow felt by the heavy impurities. These modifications were done according to [6]. Following the work done in [4] the neoclassical collisional effects were taken into account with collisions established in the frame rotating with the background ions in order to account for the effect of the diamagnetic velocity of the background ions. This effect is crucial to capture the inward flux of impurities due to the peak of the ion density and the screening effect (in the banana regime) generated by strong ion temperature gradients which are predicted by neoclassical axisymmetric theory and seen experimentally. It is important to notice that the rotation profile used was constant and equal to $\Omega = 1.2 \times 10^5 rad/s$ which is around the maximum of the experimental rotational profile. In order to use the real sheared rotation profile, modifications in the code will be taken into account in future work. In figure 4 we show the normalized flux averaged tungsten density profile at the final time of $t = 0.1s$ for 6 different cases. We notice that for both axisymmetric cases we see a localization of the peaking of impurities off-axis. For the axisymmetric case with temperature screening this localization is slightly further off the axis as expected but there is a small accumulation on axis which may be related to the fact that the density was not yet saturated at $t = 0.1s$ and therefore should be simulated during a

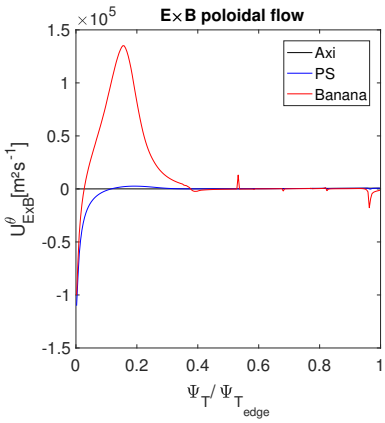

Figure 3: *Contravariant component of the poloidal $E \times B$ flow for the equilibria in 1.*

larger period of time. We also observe that strong accumulation on axis of the tungsten is observed for the 3D 1/1 kink equilibrium independently of the collisional regime. The temperature screening also seems to be not enough to generate sufficiently strong outward flux in the banana regime. However, it should be pointed out that simulations should be performed using a higher radial resolution in order to confirm robustness of these results since due to the low resolution of the VMEC radial coordinates near the axis the strong peaking is coarsely discretized. Nevertheless, these results seem to agree with the work done in [4] for the Pfirsch-Schlüter regime. In conclusion, this work has presented a self-consistent implementation of 3D centrifugal effects and electrostatic potential correction in the VENUS-LEVIS with the objective of studying tungsten accumulation in the presence of saturated internal $1/1$ kink modes in pulses similar to JET #92181. First results seem to indicate that even when including the full self-consistent 3D flows the strong accumulation of tungsten observed in [4] for the Pfirsch-Slüter regime is still observed. These results also show that in the banana regime the same strong accumulation is present in the presence of a $1/1$ internal kink. Simulations with a larger number of particles and a higher radial resolution need to be done in the future to confirm these preliminary results.

Ackowledgements

This work has been carried out within the framework of the EUROfusion Consortium and has received funding from the Euratom research and training programme 2014-2018 and 2019-2020 under grant agreement number 633053. The views and opinions expressed herein do not necessarily reflect those of the European Commission. This work was supported in part by the Swiss National Science Foundation. This work was supported by a grant from the Swiss National Supercomputing Centre (CSCS) under project ID s914 and a grant from the HPC at CINECA under project ID FUA33_SCENIC.

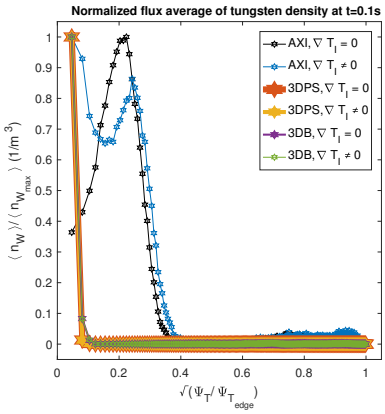

Figure 4: *Normalized tungsten flux averaged density at* $t = 0.1s$ *for different equilibria.*

References

[1] L. Garzotti et al., Nucl. Fusion **59**, 076037 (2019)

[2] T.C. Hender et al., Nucl. Fusion **56**, 066002 (2016)

[3] D.Pfefferlé et al., Computer Physics Communications **185**, 12 (2014)

[4] M. Raghunathan et al., Plasma Physics and Controlled Fusion **59**, 124002 (2017)

[5] K.C. Shaing et al., The Physics of Fluids **55**, 125001 (2015)

[6] A. J. Brizard, Phys. Plasmas **2**, 459 (1995)